Review paper

Piezoelectric energy harvester structural optimization for improving output characteristics in road environment conditions

Zhansar Z

Submitted: October 4, 2023, Revised: version 1, December 7, 2023
Accepted: January 11, 2024

Abstract
The energy dissipated as pavement vibration during daily commutes translates into significant energy lost throughout the year. From a theoretical perspective, this energy otherwise saved could go into powering streetlights or other energy-demanding facilities. This study investigated the possible implications of piezoelectric energy harvesters by finding optimal parameters in eight main categories: transducer shapes, materials, conversion modes, dimensions, external conditions influence, pavement selection, embedding methods, and protective measures. Each constituent element in the device was analyzed from a mechanical and electrical performance perspective. Recommendations on material choice for mitigating environmental factors that affect the piezoelectric effect were developed. The study compiled a custom dataset to provide a more precise view of the current state of piezoelectric research. Considering that there could be an infinite number of combinations that could be used to build transducers, which causes researchers to have diversified perspectives on optimal combinations for designing transducers, this study narrowed down possible solutions. The study developed a comprehensive understanding of all factors that must be considered while constructing the choice of a piezoelectric device and identified gaps in the current research to aid future work.

Keywords
Mechanical engineering, Piezoelectric energy harvesters, Green energy, Piezoelectric transducers, Piezoelectric devices, Road energy harvesters, Asphalt pavement, Excitation load, Excitation frequency, Mechanical response

Zhaparov Zhansar, National School Of Physics And Mathematics, Turkestan 2/1, Astana, 020000, Kazakhstan, zh.300.c@gmail.com

Introduction

In recent years, the global energy crisis and ever-increasing greenhouse gas emissions due to human high-density activity have led the scientific community to explore alternative energy harvesting solutions. Among them, solar, hydro, and wind are extensively explored ambient energy sources. Unfortunately, photovoltaic cells and wind turbines are highly dependent on intermittent ambient conditions (1), while hydroelectric power stations have a broad set of negative consequences affecting the flora and fauna (2).

The most ubiquitous ambient source is mechanical energy (3), the potential of which has not yet been fully realized. Considering the annual traffic increase in arteries and highways and the mass electrification of transport systems with a consequent substantial increase in mass road carry, technological solutions addressing mechanical energy loss during commutes are highly promising. One study estimated that 2.218×10^{16} kiloJoules are generated due to pavement deformation in the US every year and this energy remains largely unutilized (4). Road energy harvesters include photovoltaic, thermoelectric, magnetic, and piezoelectric (5, 6, 7). The most prospective mechanical transducer up-to-date is piezoelectric - its small unit dimensions, superior power density, relatively high voltage and current output compared to other energy harvesting solutions make its usable in multiple areas (8). Above all, piezoelectric devices have the potential for Weight-In-Motion systems development (9), and the mitigation of adverse vibrational effects on road integrity simultaneously (10, 11). The most significant varying parameter in piezoelectric transducers is the shape. After the basic shape is selected, its parameters can be modified according to utilization needs, which means the application of subtle changes to the structure. The factors affecting energy utilization are internal; involving dimensional optimization, as well as external, such as environmental factors like temperature and excessive stress on the pavement. Current research primarily focuses on one parameter at a time - thus, research examining the ideal combinations of multiple optimized parameters is limited. This study collates and compares optimized technical solutions from the literature and applies them coherently to create the optimized state-of-the-art piezoelectric device.

Literature Review

During the last decade, publishing activity in the field of piezoelectric transduction has significantly increased. The main focus of recent research is electrical performance optimization of piezoelectric energy harvesters. The field extends beyond transportation applications and includes smart home utilities, aerial and in-water applications, body movement, human-machine interfaces, biomedical tools, and others (12).

1. **Working principle**

The word “piezo” is derived from the Greek word *piezein*, meaning “to press tightly”. Conversion of mechanical deformation to electrical energy occurs during the compression of asymmetrical piezoelectric unit cells when individual atoms come either closer or move further away from each other, and balance is interrupted. The simplified diagram of the piezoelectric energy harvester principle is shown in Figure 1 (13). The

reverse piezoelectric effect – induced mechanical deformation of a piezoelectric material due to electric field - is also possible and used in actuator building.

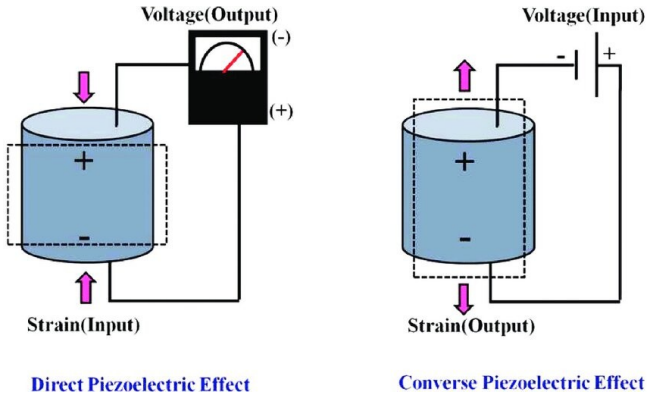

Figure 1. Simplified process of direct and converse piezoelectric effect (13).

2. Materials

The materials are divided into two categories: natural and synthetic. Ceramics and polymers are synthetic materials and have applications depending on the requirements of the field. Ceramics have close to ideal piezoelectric properties but are very brittle, while polymers are conformable but are less efficient.

Extensively utilized properties that measure performance include density (ρ), quality factor (QM), electro-mechanical coupling factor (k33), relative dielectric (κ), piezoelectric (d33) constants, and relative permittivity (ε33). Based on Table 1, the magnitude of each value of Lead zirconate titanate (PZT, ceramic) are a few orders higher than that of Polyvinylidene difluoride (PVDF, polymer) (except piezoelectric voltage coefficient (g33), which is significantly greater for PVDF). Hence, the widely adopted material in piezoelectric road technology is PZT, more precisely, its doped soft version - PZT-5H. Possessing excellent piezoelectric properties, PZT is also the most robust material ever commercially produced in the frames of the field (14). In general, there are two versions of PZT - soft and hard. Gamboa et al. (15) compared the output power of nine distinct stack PZT configurations and concluded that soft PZT with the highest piezoelectric coefficient *d33* was a top performer, outperforming both single and composite hard PZTs. Najini et al. (14) established that among PZT-4 (hard), PZT-5A (soft), and PZT-5H (soft), PZT-5H showed the best compliance in widely varying temperature and excitation frequency conditions regimes by not depolarizing. However, it is also important to note that PZT-4 has the lowest coupling effect and PZT-5H is the highest, where lower values are desirable (16).

Advancing research in PZT-5H, Wang et al. (17) conducted laboratory simulation on fatigue degradation. After a continuous load of 0.7 MPa with 10-Hertz frequency in 81 hours, the output power decreased by 96.6%. The graph of output power followed an

exponential decrease and could be expressed using Equation 1, where the coefficient of determination is 0.9888, x is the number of loadings, and y is the output power.

$$y = 4.99 + 86.62e^{(-2.55E-7)\,x} \quad \text{eq.(1)}$$

Despite substantial degradation, an important note is that, in simulations, 3 million loads were compressed into the time-frame of 81 hours - equivalent to approximately 1 year of loads on the Jintang Bridge with 4593 cars in annual average daily traffic (17). Conversely, intermittent loading had been tested 10 hours per day for 28 days. The same excitation conditions as those for the continuous load were applied. The rebound phenomenon followed each strain condition, resulting in only a 32.37% loss in output power. However, intermittent loading is not representative of real conditions, because Wang et al. (17) applied forces directly on PZT-5H piezoelectric. In practice, a protective casing is used to mitigate the concentrated load issue. For instance, Li et al. (18) studied fatigue degradation in optimized piezoelectric devices, and after 100,000 cyclic loads under 10 kN and 10 Hertz excitation parameters, no-load voltage, and power output did not decrease.

3. Transducer types

The existing transducer solutions comprise Moonie, Cymbal, Bridge, Multilayer, RAINBOW, THUNDER, Cantilever, and MF

Table 1. Comparison of piezoelectric properties between PVDF, PZT-4 and PZT-5H.

Material	ε_{33}	*Curie Temp (°F)*	g_{33}	d_{33}	k_{33}	Q_M
PVDF	8-12	176	330	-30	0.20	3-10
PZT-4	1300	716	26.1	289	0.64	500
PZT-5H	4500	392	19.7	670	0.65	70

Moonie is a bimorph structure that comprises a piezoelectric disk, typically made with PZT in the middle and metal end caps on both sides. Cymbal is an enhanced version of Moonie structure that addresses stress concentration on metal end caps that are shown in Figure 2 (19).

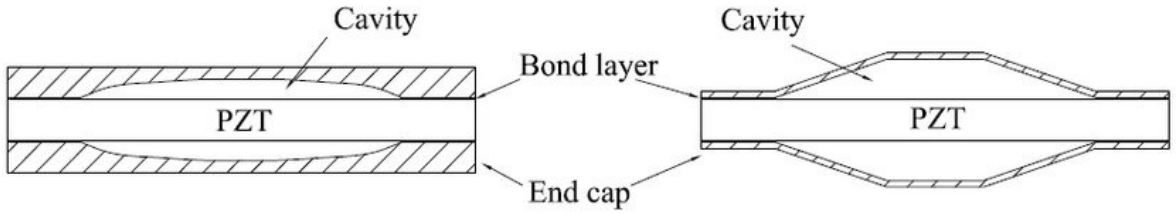

Figure 2. Scheme of Moonie (left) and Cymbal (right) (19).

Unlike Moonie, Cymbal transducers combine the longitudinal *d33* and the transverse *d31* piezoelectric strain constants. The effective piezoelectric constant is calculated by

multiplying the piezoelectric constant *d31* and M (Equation 2) and adding it to the piezoelectric constant *d33* (20). Additionally, it possesses better displacement, larger generative forces, and lower production costs (10).

$$M \cong \frac{1}{\tan(\theta)} \qquad \text{eq.(2)}$$

Bernat-Maso et al. (21) developed a cost-effective and dimension-optimized solution for Cymbals. The selected piezoelectric element was a circular membrane out of the cost and electric output considerations. The study used an unconventional method of analyzing strain on a piezoelectric patch instead of directly stating no-load voltage and power characteristics. The authors used finite element analysis (FEA) to infer that increased internal and external radii led to strain increase, while increased free height led to strain decrease. Additionally, an aluminum inner column at the center of the Cymbal allowed attaining a 10-fold increase in strain. The challenges of high mechanical energy input loss and high resonant frequency are still present. Zhao et al. (10) stated that the Bridge possessed even better electric performance, but in conditions of high excitation load (0.8 MPa), it failed due to the stress concentration and significant difference between piezo ceramic and end cap stiffness (18).

RAINBOW exerts strong piezoelectric properties but is very brittle considering its rainbow shape and piezo ceramic, which is difficult to apply to curved structure surfaces (22). From Figure 3 (23), THUNDER is an enhanced version of RAINBOW with an aluminum plate on one side and stainless steel on the other, which theoretically could be used as an energy harvester, but it has only 1 MPa of stiffness at the center point (Cymbal, for instance, has ~100 MPa) (23). Multilayer (or stack) is one of the most extensively used structure types in road piezoelectric energy harvesters studies (Figure 4) (24). The literature states that its major limitation is high stiffness, which leads to low electric energy output. To address the issue, a Cymbal-type force amplifying structure could be used (25), but in the field of road energy harvesting, high loads in the form of trucks are already present. Furthermore, stack structure has a comparatively long lifespan due to its stiffness.

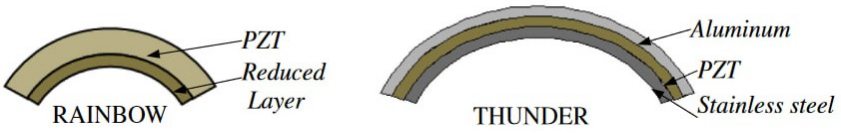

Figure 3. RAINBOW and THUNDER structures (23).

From Table 2 (23), which compares the structure types described above, it is evident that Multilayer has the highest electromechanical conversion efficiency (the highest electromechanical coupling factor (*k*), energy transmission coefficient (λmax)), and high rigidity characteristics. The one challenge that Multilayer fails to address is output energy, which is limited due to its high stiffness. Yet, in a pavement environment,

Multilayer is expected to realize its potential in high-load conditions. Even though it possesses high load compliance, it cannot withstand concentrated load, shear, and tensile stresses (26). In general, a high d33 × g33 value, low elastic compliance, and high-quality factor of piezoelectric materials are required to generate stable high output power (27, 4).

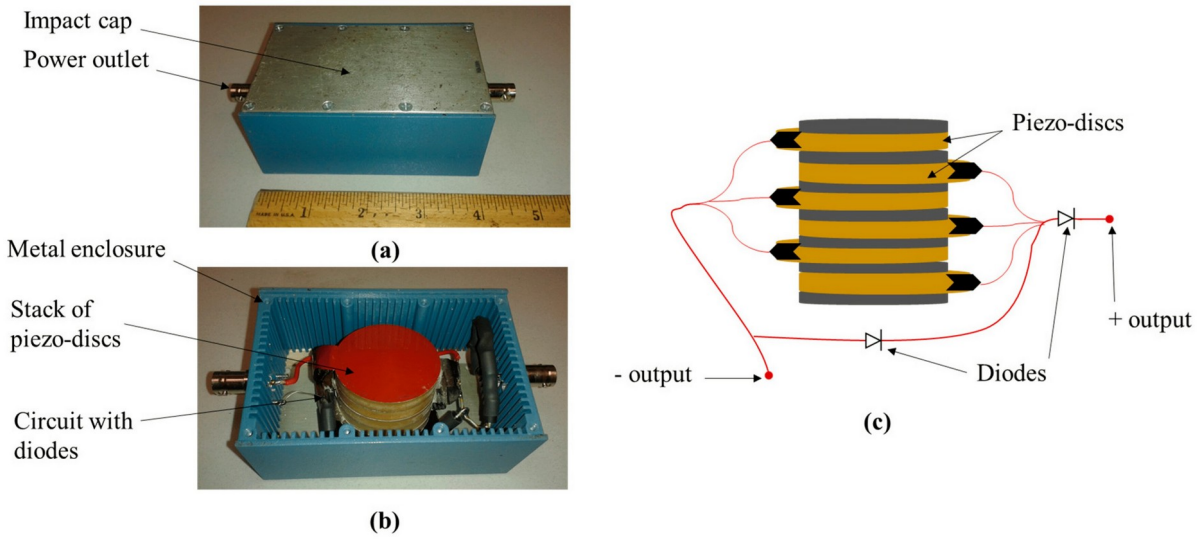

Figure 4. Stack piezoelectric structure (24).

Table 2. Comparison of transducer types based on PZT-5H using FE

Transducer	**k**	**λ_{max}**	**U_E**	**Stiffness**
Multilayer	0.75	0.282	0.03	High
THUNDER	0.74	0.237	43.38	Low
Bridge	0.29	0.057	1.13	Medium
Cymbal	0.25	0.043	0.49	Medium
MFC	0.24	0.029	0.0001	Very Low
Moonie	0.23	0.012	0.012	Medium

Another widely used piezoelectric transducer type is the cantilever beam. The standard cantilever beam for road energy harvesting purposes is shown in Figure 5 (28). This transducer type is of great interest to manufacturers and buyers because of its simple fabrication process (29). It comprises two options: unimorph and bimorph. The main difference is that the unimorph has one active and one passive layer, while the bimorph has two active layers - sandwiching a support layer, one in compression and the other in tension. The base of the cantilever beam is the support layer on which the rest of

the materials are laid, and the base is attached to the fixed block (the left side) - a static side. The main drawback of the cantilever beam is its high resonant frequency dependency. To address the issue, researchers attached a proof (seismic) mass on the substrate (30). The Proof mass functions as a medium between piezoelectric layers and excitation load - it increases flexibility in resonant frequency optimization as it can move further or closer from the fixed side. Depending on road environment conditions (i.e. high or low-speed traffic), the proof mass can be adjusted to conform to the available excitation frequency. Covering the topic of cantilever structures, Wang et al. (31) explored cantilever and rigid constraints: they determined that rigidly constrained transducers with high potential, high stress, and low electrical output for road conditions are the best. Addressing the issue of charge cancellation inherent to rigidly constrained, the authors optimized rigid cantilever beam parameters based on electrical output and stress distribution characteristics. Zhao et al. (32) proposed an optimized cantilever beam piezoelectric for low excitation frequency conditions. They analyzed the influence of substrate length, width, thickness, and seismic mass on the self-frequency of a cantilever beam. Among them, the beam length was the most influencing parameter using FEA. However, a cantilever beam type has inherent difficulty in mechanical resonance under the random impact of vehicle loads (19), which leads to the design of random vibration mitigation systems (33). It also has the highest price per bending piezoelectric patch - 6.5 and 130 times more expensive than compressive and membrane disks, respectively (21).

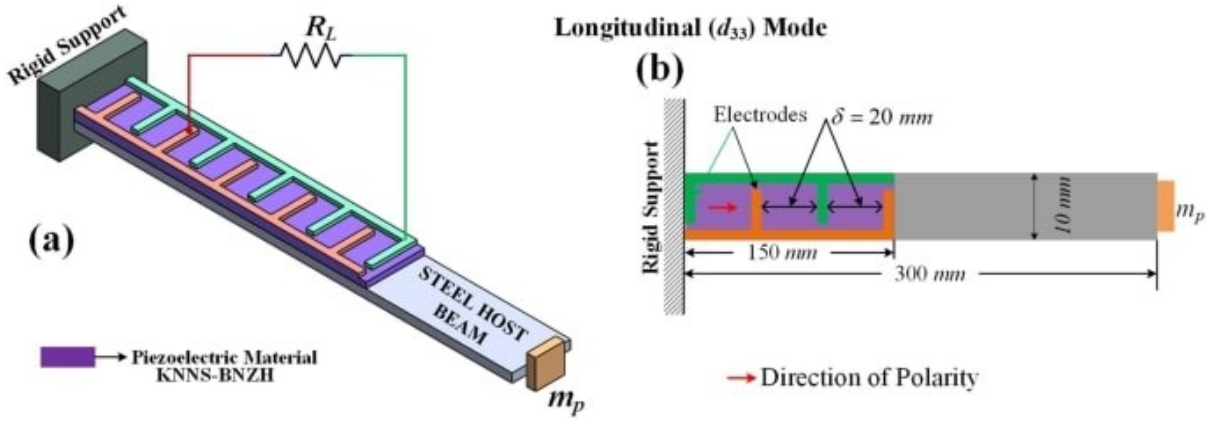

Figure 5. An example design of a bimorph cantilever beam with a proof mass (28).

4. Conversion modes

The two main conversion modes are 31 and 33 (Figure 6) (34). The modes have three indexes, 1, 2, and 3, that assign directions in the 3D space. The first and second indexes express polarization and mechanical deformation directions, respectively. For instance, 31-mode describes a transducer where the applied force is perpendicular to the induced current, while the 33-mode describes a parallel applied force. These numbers were already summarized as d, k, ε, and g coefficients in Table 1. Properties of coefficients in 33-mode are consistently 1.5 -

3 times higher than those in 31 mode, along with the much lower capacitance of the 33-mode. Furthermore, the 33-mode provides more freedom in voltage derivation since the electrodes in the 31-mode have a fixed distance between them which is determined by piezoelectric plate thickness, while in the 33-mode the distance is an independent variable (35). Thus, a piezoelectric transducer in the 33-mode is a more effective solution due to flexibility in electric performance and overall higher performance.

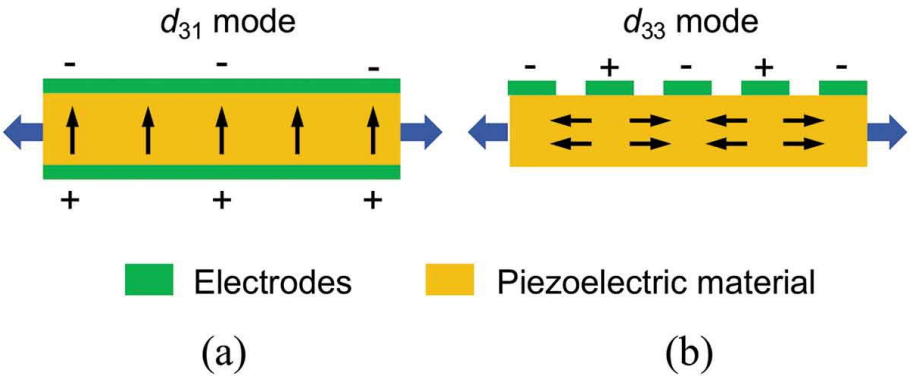

Figure 6. piezoelectric operational modes (34).

5. Unit dimensions

Depending on the chosen piezoelectric transducer type, the selection of the appropriate object dimensions to optimize for particular external conditions occurs. Wang et. al (36) established a theoretical model of stack transducers for terminal voltage and power output. The analysis showed that the greater the diameter or thickness, the smaller the peak no-load voltage and the fewer layers required to reach the optimal value. They also found that the diameter has a more significant impact on the output power, than the number of layers. At some resistance value, the terminal voltage reached its maximum and a plateau. The greater the excitation frequency, the faster it reached the plateau. Meanwhile, the output power significantly decreased after its peak value. Thus, an optimal resistance for the system existed, and this phenomenon occured when the load resistance matched the impedance of the transducer (i.e. internal resistance) (37). Relying on the impedance formula (Equation 3), where c is the internal capacitance, f excitation frequency, and R_s impedance, a higher excitation frequency leads to the earlier power peak value of the piezoelectric energy harvesters (38).

$$R_s = \frac{1}{2\pi c f} \qquad \text{eq.(3)}$$

Wang et al. (31) established a finite element model for the rigidly constrained cantilever beam. They applied a 10-Hertz vertical frequency and 1-millimeter vertical displacement with the matching external resistance (10 Hertz is ~40 miles per hour based on Table 3) (39). The authors inferred that with the increase of piezoelectric layer width, terminal voltage and output power gradually increased.

With the increase in length, output power and terminal voltage gradually decreased. Consequently, the thickness has to be as low

as possible to address high-stress conditions but not too thin for the support layer. In Figure 7, when the distance between the fixed end and piezoelectric layer is precisely 5 mm and the distance between individual layers is 6 mm, output power reaches its maximum. The impedance matching phenomenon is also consistent with this rigidly constrained cantilever beam study (31).

Table 3. Relationship between the speed of vehicles and the road vibration frequency representing the graph y=0.3x - 1.2127, where coefficient of determination is 0.8754, x is speed in miles per hour and y is frequency in hertz.

Speed (mph)	20	40	60	80	100
Frequency (Hertz)	4.79	10.79	16.79	22.79	28.79

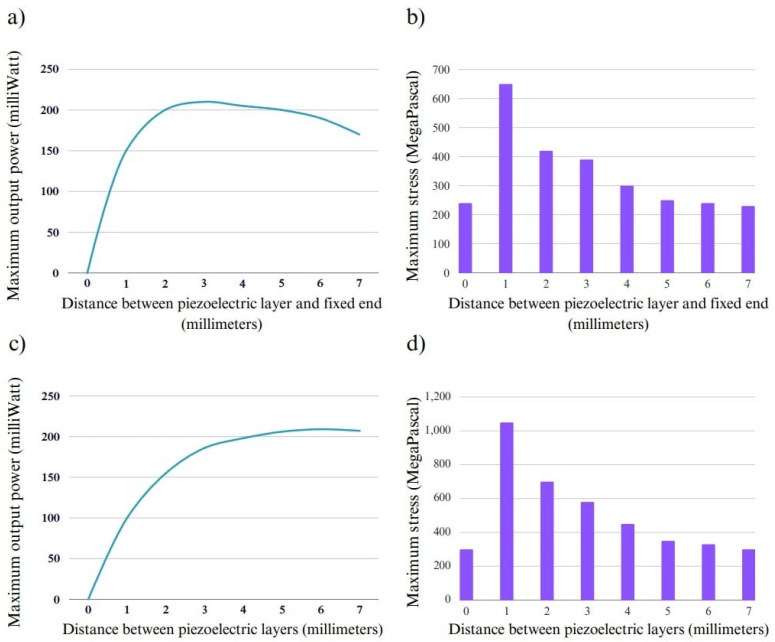

Figure 7. (a, c) maximum output power and (b, d) maximum stress depending on the distance between a piezoelectric layer and fixed end / distance between the piezoelectric layers (31).

6. External conditions

In previous studies, the load on the piezoelectric transducer is usually simplified to a half-wave sine load because the load acting on the transducer is discrete. Consequently, due to the lack of constant excitation load, the measurement of output power and voltage does not show the full piezoelectric transducer performance record. Some studies, such as those by Cao et al. (40), hence do not refer to the electrical output of different devices.

The greater the excitation load, the greater the pressure on the transducer and the higher the material utilization rate, which leads to

better electrical performance. In the case of frequency, the transducer reaches its maximum performance during resonance. This is especially significant in the case of cantilever beams with a narrow resonant operating range. Conversely, the closer the excitation frequency is to the resonant frequency, the more unstable a system is and the more it is prone to damage. The average resonant frequency of piezoelectric energy-harvesting devices is around 1 kiloHertz, while driving frequencies do not exceed the order of Hertz (41, 42). In general, Figure 8 describes the relationship between voltage, excitation frequency and load (30). The figure shows that voltage increases as loading frequency and peak loading condition increase.

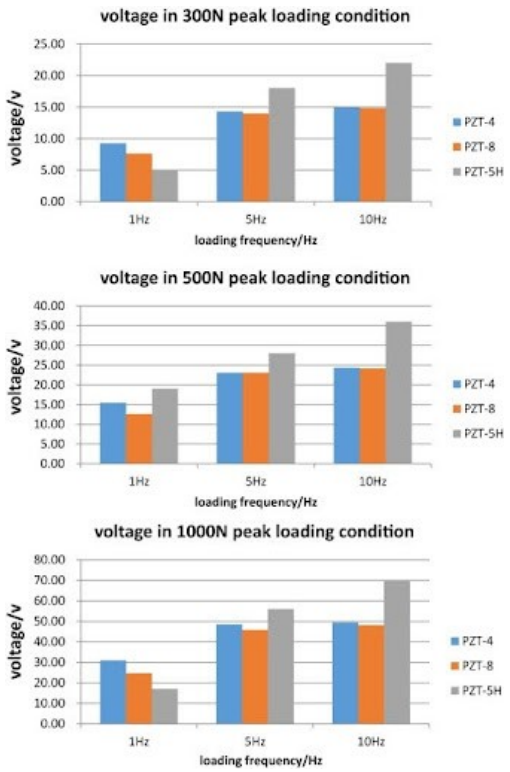

Figure 8. voltage in 300 N/500 N/1000 N peak loading condition and 1 Hz/ 5 Hz/ 10 Hz loading frequency (30).

Vertical stress is the major source of external influence, but the shear stress from vehicle acceleration and deceleration also contributes to the generated voltage. Ye et al. (43) applied horizontal shear frequency and displacement to study their influence on output power. In Figure 9, with the vertical frequency and load increased, the output power decreased slightly in both cases (43). The phenomenon can be explained by the decreased contact time between the surface and base layers due to interference from shear excitation parameters. The other important parameter that directly influences piezoelectric transducer performance is temperature. The average range of internal pavement temperature is between 5 and 130 degrees Fahrenheit, and the average change per hour is 33.8 degrees Fahrenheit (44). Yang et al. (45) explored the influence of

temperature on output characteristics. High temperatures negatively affected no-load voltage and electric energy, with a 38% decrease in voltage during the transition from 5 to 86 degrees Fahrenheit. However, electric energy output in the same temperature range had a 25% increase, as shown in Figure 10 (45). The reasoning behind the phenomenon is an increase in energy output efficiency that consequently increases ultimate electric energy output. Moreover, since the charge per unit area in piezoelectric transducers increases with temperature, the piezoelectric coefficient d_{33}, being directly proportional to the charge (as shown in Equation 3), also increases. Meanwhile, Wang et al. (46) established that relative permittivity ε_{33} approximately linearly increases with temperature. Furthermore, Cao et al. (47) found that the output power for piezoelectric ceramics also increases with the temperature. All three studies mentioned here showed consistent results on the effect of temperature on voltage and energy generation results.

7. Pavement materials

Pavement parameters include materials constituting the surface, base, sub-base, cushion, and sub-grade courses. The most commonly used type of surface layer is asphalt concrete from crushed aggregate and bitumen. Bitumen prevents dust from accumulating in the pores of the asphalt and provides enhanced waterproofing, increasing the lifespan of the surface layer and providing a protective casing for piezoelectric devices. Two combinations can be studied: AC13 in combination with AC20 or AC16 in combination with AC20. The numbers refer to the nominal maximum aggregate radius in millimeters. Thus, AC13 has the smallest particles and the largest number of contact forces (48). AC16 combined with AC20 is highly favorable since it shows a substantial gap in output characteristics compared with AC13 (700% gain under 0.95 kN) because of larger particles that facilitate force transmission (49).

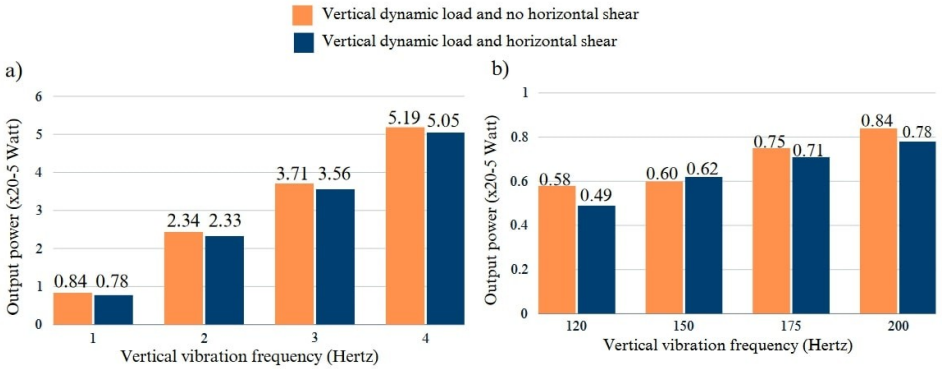

Figure 9. Electrical response of piezoelectric energy harvester under combined vertical vibration and horizontal shear: (a) influence of vertical load on output performance and (b) influence of vibration frequency on output performance. Adapted from Ye et al. (43)

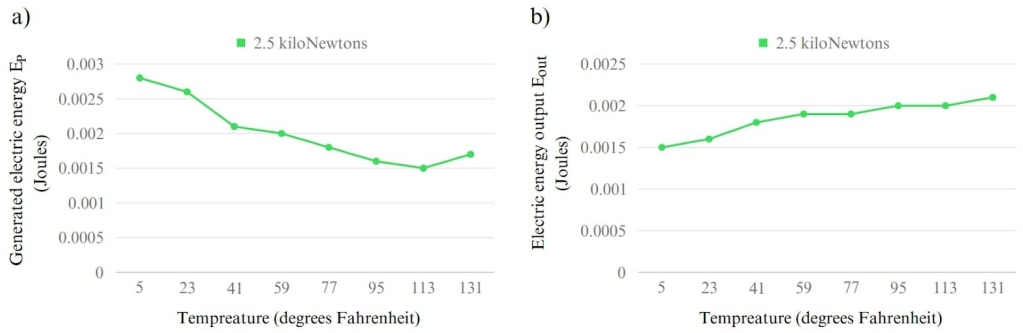

Figure 10. (a) the generated electric energy in relation to temperature (b) the output electric energy in relation to temperature. Adapted from Yang et al. (45)

It is also necessary to address the challenge of stiffness difference, which can lead to a bonding failure of the device-pavement interface and uncoordinated deformation of the device-pavement composite structures (48). Thus, the closer the pavement is in deformation displacement value (or elastic modulus) to the device, the higher are the coupling properties (9). Regarding the base layer, different configurations exist: rigid, flexible, and combined pavement. In general, the rigid pavement configuration has the greatest deformation compliance, while the flexible configuration has the least deformation compliance (50). However, stress distribution changes in the base course do not affect the device since its location is in the upper layer. However, they do affect the base course since all the changes occur within the first three pavement layers (51).

The thickness of each pavement layer depends on the sub-grade layer bearing capacity and traffic loading (52). The lower the sub-grade strength and the higher the applied load, the thicker the layers must be. Bezabih et al. (52) found that flexible pavements were more economical for lower traffic capacities.

8. Embedding in pavement

Cao et al. (47) defined two main methods of piezoelectric device embedding into the pavement process: placement of the device inside the ready pavement or laying the pavement with the device. In the first method, grooves are applied, and joints are grouted with asphalt mortar. Hence, the transducer is not subject to high-temperature processes, but the pavement integrity is disrupted. In this case, the protective shell is of good use in temperature deviation protection throughout the operating lifetime and initial preparation (44). In the second method, piezoelectric devices are initially scattered on the base layer, and then pavement is laid. This is a feasible solution considering transducer degradation is less than 35% after three years of PZT-5H application (44).

To maximize the piezoelectric transducer utilization rate, it is also necessary to address the relative placement and dimensions of the device. These dimensions depend on the tire contact area, which is represented by two semicircles with two rectangles on both ends, but to simplify, researchers assume a rectangle with an equivalent area (53). The contact area must be calculated according to the selected tire inflated pressure, excitation

frequency, and axial load parameters (54). Wang et al. (26) elaborated on the topic of vehicles' contact dimensions based on typical loadings and tire types, where tire tread width equals transverse grounding width. The length is two times higher while the width is almost equal for an average truck compared with an average car. Thus, based on the tires' contact area, by layout of the transducers inside the device, manufacturing costs, and construction convenience, Wang et al. (26) inferred that the optimal dimensions for cars and trucks are, respectively, 100 × 100 mm^2 and 150 × 150 mm^2 with an approximate spacing of 365 and 545 millimeters. However, the setup is established for direct contact with vehicle tires, which in turn maximizes strain transfer (55, 32), but it is recommended to place the device at a depth of 25 - 50 millimeters to provide unimpeded pavement rehabilitation and protection to a piezoelectric device (56). Placing the device inside the pavement leads to stress dissipation through the particle structure of the asphalt concrete.

9. Protective casing

Recent research on piezoelectric energy harvesters in road applications elaborates on protective shells for units since appropriate shell design can facilitate piezoelectric properties by amplification of stress, coordinated deformation with the adjacent pavement layer, and thermal and hydrological protection of the transducer. Many different energy harvester structures have been proposed, but most follow the same pattern; consisting of a bearing plate, a piezoelectric layer, and the base.

The two basic shapes of the protective shell can be either square or round, which leads to different mechanical responses of the pavement. When the tire entirely covers the area of a device, the yield stress and side shear stress of the circular device are ~125% and ~116% of a square device, respectively (57). On the other hand, the compressive stress of the pavement at the bottom of the device is generally slightly higher, which is conducive to increased electric output (57). Yang et al. (58) built a stack unit-based piezoelectric device (Figure 11). The authors used stack PZT-5H as a transducer with a total of 19 placement holes in the nylon positioning plate. Polyamide 66 (PA66) with glass fiber for plastic strengthening was constructed for the bearing plate and base. The researchers concluded that a square shape was more compatible with tire contact patches on the road while conducting less compressive stresses on the lowest AC layer (51). The force applied on the bearing plate was channeled downwards to the stainless steel electrode. Yang et al. (58) considered environmental insulation using a waterproof gasket made from silica gel.

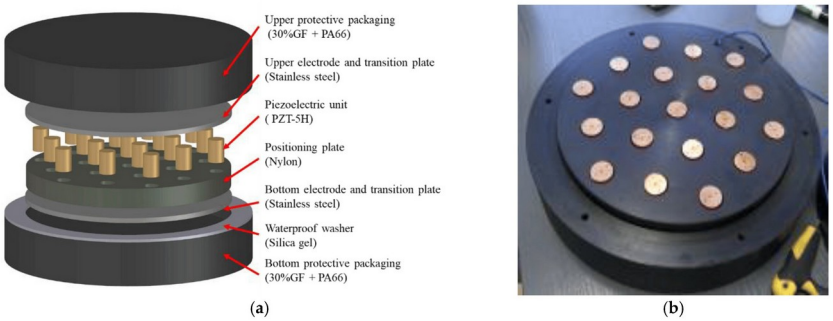

Figure 11. Example of a unit-based piezoelectric device (58).

Another example is a pile unit-based energy harvester but with more technical considerations in mind (49). Li et al. (49) applied silicone for a positioning plate and utilized protective gaskets on the transducer. A rubber sponge and glass adhesive were utilized for environmental insulation. Some studies applied single structured units (cylindrical PZT) (15, 16, 58, 59). However, most of them used composite transducers (stack PZT) because composite structures provided better electromechanical conversion efficiencies (15). Circular, square, hexagonal, and octagonal are all possible shapes for the transducer to take since they have the same output power, but the induced stress of the circular transducer is the lowest (16). For single structures, the electric performance of the single Φ6 × 10 mm^2 piezoelectric material is considerably higher than that of the Φ35 × 2 mm^2 piezoelectric material based on finite element analysis (59).

For composite structures, the output power and voltage of an array-based device are significantly greater than that of a stack-based device (60). Stacked transducers could achieve the maximum of 5-milliWatt power, while arrays could achieve 160-milliWatt power in parallel connections.

Furthermore, structuring a smaller cross-sectional area of the stack transducer, making it Φ15.87 × 31.76 mm^2, significantly increased the overall electric performance in comparison with a stack transducer of dimensions Φ25.20 × 12.60 mm^2 (58). The same applies to array-based transducers, where a smaller cross-sectional area, that is lower in the number of units, leads to higher power output with the compromise in structural stability (60). Combining the results from the studies above, making a round stack transducer with a smaller diameter and more considerable height and placing it in an array-based device could potentially enable the positive effects of both high stack strength and high array-based power generation.

When selecting the outer shell material (bearing plate and base), metal is an excellent choice, as it possesses high strength and prominent modulus characteristics. However, it has poor weathering ability, and high thermal and electrical conductivity, which does not respond to piezoelectric transducer insulating requests. Moreover, metals like aluminum alloy and stainless steel possess low coupling effects due to significant Young's modulus difference (61). It is also recommended to have a lower elastic

modulus to have higher compressive stress (62). On the other hand, engineering plastics have high abrasion and chemical resistance, high impact strength, and low thermal and electrical conductivity. Among engineering plastics, Polyamide 11 is derived using renewable sources (castor oil plants) and has outstanding mechanical properties; Polyamide 12, in general, has similar properties as Polyamide 11 and can be derived from both petroleum and renewable sources; Polyamide 46 has outstanding fatigue resistance; and Polyphthalamide possesses excellent stiffness and strength characteristics (63, 64). However, they have drawbacks of complex production stages and consequent expensive prices. For that reason, Nylon 6 and Nylon 66 are the most widely used engineering plastics worldwide (63). Nylon is the most suitable material for pavement applications as it has the closest to pavement elastic stiffness and is comparatively lightweight. Some authors use 30% glass fiber reinforced Polyamide 66 (PA66-GF30), where 66 refers to monomers adipic acid and hexamethylenediamine. Compared to conventional Polyamide 66, the 30% glass fiber reinforcement increases strength by 18%, stiffness by 52%, and overall dimensional stability while maintaining a relatively low price (65, 66).

Other researchers have used MC Nylon, monomer-cast nylon, which is chemically the same as Nylon 6 but has better mechanical properties, chemical resistance, abrasion resistance, and corrosion resistance. Moreover, PA66-GF30 and Nylon 6 have excellent machinability - an important property for enabling mass-production (67).

Regarding positioning plates, scientists continue using the same materials applied for the bearing and base layers. However, this is not necessary since the purpose of the positioning plate is to fix the transducers in place; therefore, they are not subject to high loads and do not require materials with a high elastic modulus. Sherren et al. (68) proposed that PLA plastic is sufficient for this purpose.

Since piezoelectric energy harvesters' operating environment includes constant random excitation conditions, an opposite voltage may be generated by PZTs. Thus, previous research has used diode rectifiers in each unit for electric output maximization (68). Figure 12 shows the Full-bridge - the most commonly used diode rectifier type (69). However, Edla et al. (70) pointed out the inability of the Full-bridge diode rectifier type to work in low-voltage conditions and proposed a low-loss hybrid AC–DC rectification technique that uses magnets and reed switches with conventional semiconductor diodes. Other solutions frequently include MOSFETs, which are used to achieve higher voltage and efficiency yet are not self-powered (71). Schlichting et al. (68) addressed this issue and constructed a self-powered rectifier, substituting diodes for MOSFETs and adding a capacitor (Figure 13). This design is set up for high-frequency and low amplitude environments, which coincides with stack piezoelectric's small displacement and road's high-frequency requests, making it suitable for highway application.

To provide a stable and fuel-efficient ride, it is desirable to diminish the sinking displacement, which occurs when a piezoelectric device is being compressed (39). Cao et al. (40) found that by increasing the pre-load on a piezoelectric device, its

sinking displacement significantly decreases without considerable electric energy loss. Additionally, a pre-load force can induce the resonant frequency to change. In a study by Hu et al. (72), a stretching preload of 50 N induced the resonant frequency of the piezoelectric bimorph to increase from 129.3 to 169.4 Hertz, while a compressive pre-load of 50 N decreased the resonance from 129.3 to 58.1 Hertz. However, considering that the cross-sectional area of a piezoelectric device is 150 x 150 * 10^{-6} m^2, the average density of AC20 is 1,022 Kg/m^3 (73), and the approximate burying depth is 50 * 10^{-3} m, the pre-load force exerted on the device by the pavement is approximately 11.5 N. Thus, the force from a pavement is too low to be used as a pre-load, and in future studies, a design allowing pre-load might be beneficial to develop.

Despite coordinated stress deformation due to the bearing plate, additional protection from stress attenuation on piezoelectric transducers and side walls is desirable. Wang et al. (61) found that a filet pad with a thickness and filet size of 3 millimeters is optimal for a Φ30 x 15 mm^2 piezoelectric unit due to approximately uniform distribution of top compressive and von Mises stresses. They also proposed a material with elastic modulus between 8 - 15 GPa for the best piezoelectric performance.

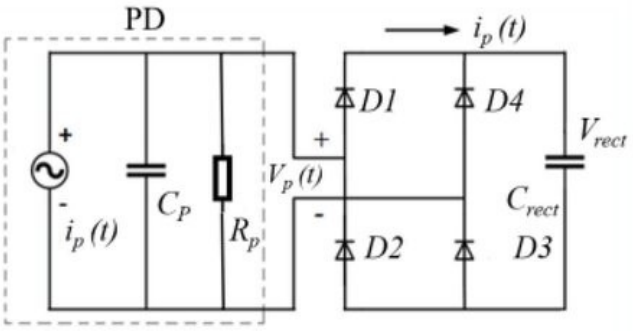

Figure 12. Full-bridge diode rectifier circuit diagram (PD - piezoelectric device) (69).

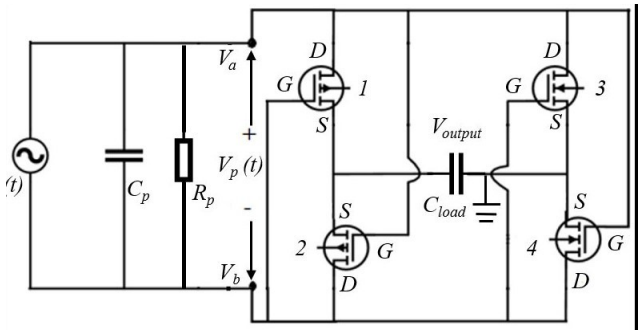

Figure 13. self-powered H-bridge rectifier circuit diagram (69).

One of the emerging challenges is the loss of carrying load due to applied force acting on the device side instead of on the piezoelectric layer, consequently diminishing electric

output characteristics. Cao et al. (47) developed a concept of a full-pressure energy harvester, where the bearing plate is placed in the base. The concept results were very promising, with a 100% utilization rate. However, the authors did not develop a waterproof design, which would require complex sealing due to direct contact with the piezoelectric but enhance the practical applications of this technology.

Regarding the sealing itself, most authors used silicone rubber (19, 51, 62, 74). In comparison with neoprene rubber, it is cheaper and more flexible. Another alternative is ethylene propylene diene monomer (EPDM) rubber presented in Table 4, which is comparable to silicone rubber and even possesses temperature insulation properties but cannot withstand high temperatures. Table 4 shows the properties of three types of rubber: neoprene, silicone, and EPDM. From the viewpoint of distinct characteristics, silicone rubber has a wide operational range, while neoprene has excellent resistance to chemicals (which is not required in pavement conditions). On the other hand, EPDM has the lowest price among the three types of rubber, is a temperature insulator, and is resistant to repeated shocks. Thus, EDPM may be a better solution than silicone and neoprene rubbers for piezoelectric transducer insulation.

Table 4. Insulating materials' mechanical and chemical properties

Property	*Neoprene Rubber*	*Silicone Rubber*	*EPDM Rubber*
Weather & UV Resistance	Resistant to weather and UV radiation	Resistant to weather and UV radiation	Resistant to weathering, ozone, and UV radiation
Chemical Resistance	Moderate resistance to chemicals, oils, acids	Moderate resistance to chemicals, oils, acids	Good resistance to water, chemicals, and solvents
Tensile Strength	3.5 - 20.1 MPa	1.4 - 10 MPa	3.5 - 17 MPa

Discussion

Regarding the materials, PZT is described as highly robust (14). Specifically, PZT-5H is highly promising for widespread use due to its compliance with varying temperature and excitation frequency conditions by not depolarizing. The second parameter explored was transducer shapes. Multilayer has the highest electromechanical conversion efficiency (electromechanical coupling factor (k), energy transmission coefficient (λ_{max}), medium output energy (U_E)), and high rigidity characteristics. This shape does not possess high load compliance, implying that it cannot withstand concentrated load, shear, and tensile stresses (25). In situations where engineers prefer a shape that can withstand these conditions, the cantilever beam may be a better, albeit a more expensive, option (21). Among Multilayer alternatives, MFC and THUNDER have the lowest stiffness and are prone to critical damage under pavement conditions (22), while the Bridge alternative has stress attenuation issues (10), but the Cymbal alternative has close to Multilayer properties and also works under higher loads and also is less stiff (21). Considering conversion modes, the 33 mode is the most

compatible with pavement utilization. Properties of coefficients in 33-mode are consistently 1.5 - 3 times higher than those in 31-mode. Additionally, electrodes in 33-mode are not thickness-dependent, allowing for a flexible piezoelectric setup (34). The load on the piezoelectric transducer is usually simplified to a half-wave sine load. Thus, the excitation parameters are investigated from load and frequency variables. It is essential to match internal and external resistance, where the former depends on excitation frequency and internal capacitance. The greater the excitation load, the greater the pressure on the transducer and the higher the material utilization rate, which leads to better electrical performance. In the case of frequency, the transducer reaches its maximum performance at resonant frequency. However, the average resonant frequency of piezoelectric transducers is around 1 kiloHertz, while driving frequencies do not exceed the order of Hertz (41, 42). This challenge makes addressing resonant frequency decrease during pre-load relevant for study in further research (72). It is also important to build a thermally insulating device to optimize only for one piezoelectric condition, as low to high temperatures transition negatively affects no-load voltage and electric energy while positively affecting the charge per unit area piezoelectric coefficient d33, relative permittivity ε_{33}, and power output (45, 46, 47).

Regarding pavement materials, AC13, AC16, and AC20 types exist. AC13 has the smallest particles and the highest number of contact forces (48). At the same time, AC16 combined with AC20 is highly favorable since it shows a substantial gap in output characteristics compared with AC13 (700% gain under 0.95 kN) because of larger particles that facilitate force transmission (47). The base course's influence is negligible on piezoelectric characteristics and can be neglected (51).

Considering the placement of the device, the contact area consideration is paramount. The contact area must be calculated according to the selected tire inflated pressure, excitation frequency, and axial load parameters (54). According to Wang et al. (26), based on the tires' layout of the transducers inside the device, manufacturing costs, and construction convenience, the optimal dimensions for cars and trucks are 100 mm × 100 mm and 150 mm × 150 mm with approximate spacing of 365 and 545, respectively. Regarding highways, the latter set of dimensions is the best choice as most of the traffic consists of trucks or large vehicles.

Furthermore, the device must lie at a depth of 25 - 50 millimeters to provide unimpeded pavement rehabilitation and protection for a piezoelectric device (56). After the placement, the embedding methodology needs to be selected. Embedding the harvester into the ready pavement is safe for piezoelectric transducer integrity; however, it makes for less coupling with pavement and demands higher processing costs. Hence, the method of pavement and devices' simultaneous layout is better, but the protective casing must be designed accordingly. In addition to the thermal and hydrological protection of the transducer, the protective shell facilitates piezoelectric properties by amplification of stress and coordinate deformation with the adjacent pavement layer. For the bearing plate, it is recommended to use PA66 for its

comparatively low elastic modulus difference with the pavement and above average compressive and tensile strengths. The number of devices must be low to reach a higher voltage and energy output (58), but not too low to compromise structural integrity (4 - 9 piezoelectric units). The positioning plate could be made out of PA6, which is characterized by lower resistance to repeated shocks compared to PA66. All piezoelectric units must be intertwined using parallel copper electrodes, and each transducer must be connected to a separate rectifier for efficient AC to DC conversion (75).

Concerning the single unit, the stack structure with a smaller cross-sectional area and more individual layers with greater thickness should be considered (34). Regarding piezoelectric insulation, EPDM is an economically feasible solution, which can act both as waterproofing and heat-insulating material, having properties applicable to the pavement conditions.

The Table in the Appendix reviews the current state of the piezoelectric energy harvesting field with a focus on Stack PZT-5H transducers, as they are the most promising type based on the results of this review.

Conclusion

This study reviewed transducer shapes, materials, conversion modes, external and internal influence parameters, placement in pavement, pavement selection, and protective measures. The study then proposed an optimized transducer based on synthesized literature, with approximate numerical size ranges for other authors to adjust parameters according to their needs. The aspects of piezoelectric devices are optimized up to date, but after some time, an innovation in one of the transducer types could make findings obsolete and diminish the value of this paper. However, this paper calls attention to the need for the universality of every piezoelectric energy harvester's aspects by finding optimal solutions in each area of piezoelectric study. The results of this study could facilitate progress since many optimal solutions exist but are not universal because there are few studies that examine the combined impact of multiple parameters.

Amidst pursuing a solution in one area, most authors omit the other: neglecting tires' grounding area, environmental influence, or materials. However, the investigation has stated a smaller area is more electrically beneficial but more prone to damage; it is irrational to measure performance on a shear unprotected piezoelectric disk; every material, and even its shape, has its own limitation.

Hence, this study provides a comprehensive synthesis of individual design and material elements of piezoelectric transducers in such a way that enables future research to expand and build upon nuanced relationships between these parameters. Furthermore, the protective casing is yet to expand as it is barely investigated, accounting for a lack of thorough explanations from most researchers for the material choice. Looking at how changing dimensions alternate the electromechanical response of the transducer, the device as a whole, and the layer adjacent to the device is necessary. Further research into piezoelectric properties can ultimately

lead the piezoelectric technology to be economically feasible to establish in widespread pavement applications.

Acknowledgments

I sincerely thank my mentor, Adair Garrett, for guiding me through the paper-writing process.

References

1. Albadi, M.H. and El-Saadany, E.F. Overview of wind power intermittency impacts on Power Systems. Electric Power Systems Research, 80(6): 627–632, 2010. https://doi.org/10.1016/j.epsr.2009.10.035.

2. Arantes, C.C. et al. Impacts of hydroelectric dams on fishes and fisheries in tropical rivers through the lens of functional traits. Current Opinion in Environmental Sustainability, 37: 28–40, 2019. https://doi.org/10.1016/j.cosust.2019.04.009.

3. Bin Ab Rahman, M.F. and Kok, S.L. Investigation of useful ambient vibration sources for the application of energy harvesting, *2*011 IEEE Student Conference on Research and Development [Preprint]. https://doi.org/10.1109/SCOReD.2011.6148771.

4. Xiong, H. and Wang, L. Piezoelectric Energy Harvester for public roadway: On-site installation and evaluation. Applied Energy, 1z: 101–107, 2016. https://doi.org/10.1016/j.apenergy.2016.04.031.

5. Jiang, W. *et al.* Energy harvesting from asphalt pavement using thermoelectric technology, Applied Energy, 205: 941–950, 2017. https://doi.org/10.1016/j.apenergy.2017.08.091.

6. Calautit, K., Nasir, D.S.N.M. and Hughes, B.R. Low power energy harvesting systems: State of the art and future challenges. Renewable and Sustainable Energy Reviews, 147: 111230, 2021. https://doi.org/10.1016/j.rser.2021.111230.

7. Zhang, Y. *et al.* Simulation and experimental study on the energy performance of a pre-fabricated photovoltaic pavement. Applied Energy, 342: 121122, 2023. https://doi.org/10.1016/j.apenergy.2023.121122.

8. Toprak, A. and Tigli, O. Piezoelectric Energy Harvesting: State-of-the-art and challenges. Applied Physics Reviews, 1(3): 031104, 2014. https://doi.org/10.1063/1.4896166.

9. Zhao, Q. *et al.* Development of a novel piezoelectric sensing system for Pavement Dynamic Load Identification. Sensors, 19(21): 4668, 2019. https://doi.org/10.3390/s19214668.

10. Zhao, H., Yu, J. and Ling, J. Finite element analysis of cymbal piezoelectric transducers for harvesting energy from asphalt pavement. Journal of the Ceramic Society of Japan,

118(1382): 909–915, 2010. https://doi.org/10.2109/jcersj2.118.909.

11. Hagood, N.W. and von Flotow, A. Damping of structural vibrations with piezoelectric materials and passive electrical networks. Journal of Sound and Vibration, 146(2): 243–268, 1991. https://doi.org/10.1016/0022-460X(91)90762-9

12. Sezer, N. and Koç, M. A comprehensive review on the state-of-the-art of Piezoelectric Energy Harvesting. *Nano Energy,* 80: 105567, 2021. https://doi.org/10.1016/j.nanoen.2020.105567.

13. Mishra, S. *et al.* Advances in piezoelectric polymer composites for energy harvesting applications: A systematic review. Macromolecular Materials and Engineering, 304(1): 1800463, 2018. https://doi.org/10.1002/mame.201800463.

14. Najini, H. and Muthukumaraswamy, S.A. On generation of renewable energy from Road Traffic. International Journal of Sustainable Energy and Environmental Research, 5(2): 14–30, 2016. https://doi.org/10.18488/journal.13/2016.5.2/13.2.14.30.

15. Gamboa, B., Bhalla, A. and Guo, R. Assessment of PZT (soft/hard) composites for energy harvesting. Ferroelectrics, 555(1):118–123, 2020. https://doi.org/10.1080/00150193.2019.1691389.

16. Niasar, E.H., Dahmardeh, M. and Googarchin, H.S. Roadway Piezoelectric Energy Harvester design considering electrical and mechanical performances. Proceedings of the Institution of Mechanical Engineers, Part C: Journal of Mechanical Engineering Science, 234(1), pp. 32–48, 2019. https://doi.org/10.1177/0954406219873366.

17. Wang, J. *et al.* Experimental study on fatigue degradation of piezoelectric energy harvesters under equivalent traffic load conditions. International Journal of Fatigue, 150: 106320, 2021. https://doi.org/10.1016/j.ijfatigue.2021.106320.

18. Li, C. *et al.* Development and piezoelectric properties of a stack units-based piezoelectric device for roadway application. Sensors, 21(22): 7708, 2021. https://doi.org/10.3390/s21227708.

19. Wang, W., Jiang, Y. and Thomas, P.J. Structural design and physical mechanism of axial and radial sandwich resonators with Piezoelectric Ceramics: A Review. Sensors, 21(4): 1112, 2021. https://doi.org/10.3390/s21041112.

20. T.-B. Xu. Energy harvesting using piezoelectric materials in aerospace structures. Structural Health Monitoring (SHM) in Aerospace Structures, 7: 175-212, 2016. https://doi.org/10.1016/B978-0-08-100148-6.00007-X.

21. Bernat-Maso, E. *et al.* Energy harvester based on low cost piezoelectric membrane for road traffic application. Microsystem Technologies, 29(7): 985–998, 2023.

https://doi.org/10.1007/s00542-023-05490-1.

22. Jiang, S. *et al.* Properties of novel 0–3 PZT/silicone resin flexible piezoelectric composites for ultrasonic guided wave sensor applications. Frontiers in Materials, 9, 2022. https://doi.org/10.3389/fmats.2022.958775.

23. Zhao, H., Ling, J. and Yu, J. A comparative analysis of piezoelectric transducers for harvesting energy from asphalt pavement. Journal of the Ceramic Society of Japan, 120(1404): 317–323, 2012. https://doi.org/10.2109/jcersj2.120.317.

24. Walubita, L. *et al.* Prospective of societal and environmental benefits of piezoelectric technology in road energy harvesting. Sustainability, 10(2): 383, 2018. https://doi.org/10.3390/su10020383.

25. Kuang, Y., Daniels, A. and Zhu, M. A sandwiched piezoelectric transducer with flex end-caps for energy harvesting in large force environments. Journal of Physics D: Applied Physics, 50(34): 345501, 2017. http://dx.doi.org/10.1088/1361-6463/aa7b28.

26. Wang, C. *et al.* Optimization design and experimental investigation of piezoelectric energy harvesting devices for Pavement. Applied Energy, 229: 18–30, 2018. https://doi.org/10.1016/j.apenergy.2018.07.036.

27. Li, L. et al. Recent progress on piezoelectric energy harvesting: Structures and materials. Advanced Composites and Hybrid Materials, 1(3): 478–505, 2018. https://doi.org/10.1007/s42114-018-0046-1.

28. Mouapi, A., Hakem, N. and Kandil, N. Cantilevered piezoelectric micro generator design issues and application to the mining locomotive. Energies, 13(1): 63, 2019. https://doi.org/10.3390/en13010063.

29. Varadha, E. and Rajakumar, S. Performance improvement of piezoelectric materials in energy harvesting in recent days – a review. Journal of Vibroengineering, 20(7): 2632–2650, 2018. https://doi.org/10.21595/jve.2018.19434.

30. Xu, X. *et al.* Application of piezoelectric transducer in energy harvesting in Pavement. International Journal of Pavement Research and Technology, 11(4): 388–395, 2018. https://doi.org/10.1016/j.ijprt.2017.09.011.

31. Wang, C. *et al.* Structure optimization and performance of Piezoelectric Energy Harvester for improving road power generation effect. Energy, 270: 126896, 2023. https://doi.org/10.1016/j.energy.2023.126896.

32. Zhao, H., Qin, L. and Ling, J. Synergistic performance of piezoelectric transducers and asphalt pavement. International Journal of Pavement Research and Technology, 11(4): 381–

387, 2018. https://doi.org/10.1016/j.ijprt.2017.09.008.

33. Zhai, J., Shang, L. and Zhao, G. Topology optimization of piezoelectric curved shell structures with active control for reducing random vibration. Structural and Multidisciplinary Optimization, 61(4): 1439–1452, 2019. https://doi.org/10.1007/s00158-019-02423-3.

34. Hiroshi Toshiyoshi, Suna Ju, Hiroaki Honma, Chang-Hyeon Ji & Hiroyuki Fujita. MEMS vibrational energy harvesters. Science and Technology of Advanced Materials, 20(1): 124-143, 2019. https://doi.org/10.1080/14686996.2019.1569828.

35. Kim, S.-B. *et al.* Comparison of MEMS PZT cantilevers based on d31 and d33 modes for vibration energy harvesting. Journal of Microelectromechanical Systems, 22(1): 26–33, 2013. https://doi.org/10.1109/JMEMS.2012.2213069.

36. Wang, S. *et al.* Size effect of piezoelectric energy harvester for road with High Efficiency Electrical Properties. Applied Energy, 330: 120379, 2023 https://doi.org/10.1016/j.apenergy.2022.120379.

37. Anton, S.R. and Sodano, H.A. A review of power harvesting using piezoelectric materials (2003–2006). Smart Materials and Structures, 16(3), 2007. http://dx.doi.org/10.1088/0964-1726/16/3/R01.

38. Wang, P. *et al.* Output optimization of piezoelectric monitoring system considering loss impedance and spatial arrangement under Traffic Load. Transportation Geotechnics, 36: 100820, 2022. https://doi.org/10.1016/j.trgeo.2022.100820.

39. Song, Y. *et al.* Road energy harvester designed as a macro-power source using the piezoelectric effect', *International Journal of Hydrogen Energy*, 41(29): 12563–12568, 2016. https://doi.org/10.1016/j.ijhydene.2016.04.149.

40. Cao, Y., Sha, A., *et al.* Energy output of piezoelectric transducers and pavements under simulated traffic load. Journal of Cleaner Production, 279: 123508, 2021. https://doi.org/10.1016/j.jclepro.2020.123508.

41. Chen, C. *et al*. A high density piezoelectric energy harvesting device from highway traffic — system design and Road Test', Applied Energy, 299: 117331, 2021. https://doi.org/10.1016/j.apenergy.2021.117331.

42. Wang, Chaohui, Shuai Wang, et al. "Fabrication and performance of a power generation device based on stacked piezoelectric energy-harvesting units for pavements." *Energy Conversion and Management*, vol. 163:. 196–207, 2018. https://doi.org/10.1016/j.enconman.2018.02.045.

43. Ye, F. *et al.* Research on integrated electrical and mechanical response of piezoelectric

asphalt pavement material under bidirectional cyclic loads. SSRN Electronic Journal [Preprint], 2022. http://dx.doi.org/10.2139/ssrn.4159306.

44. Wang, C. *et al.* Design and testing of road piezoelectric power generation device based on traffic environment applicability. Applied Energy, 299: 117344, 2021. https://doi.org/10.1016/j.apenergy.2021.117344.

45. Yang, H., Guo, M., *et al.* Investigation on the factors influencing the performance of Piezoelectric Energy Harvester. Road Materials and Pavement Design, 18(3): 180–189, 2017. https://doi.org/10.1080/14680629.2017.1329873.

46. Wang, D., Fotinich, Y. and Carman, G.P. Influence of temperature on the electromechanical and fatigue behavior of Piezoelectric Ceramics. Journal of Applied Physics, 83(10): 5342–5350, 1998. https://doi.org/10.1063/1.367362.

47. Cao, Y. *et al.* Energy harvesting performance of a full-pressure piezoelectric transducer applied in pavement structures. Energy and Buildings, 266: 112143, 2022. https://doi.org/10.1016/j.enbuild.2022.112143.

48. He, J., Xiao, H. and Chen, X. Homogeneity of asphalt mixture at mesoscopic level based on DEM simulation and low-temperature splitting test. International Journal of Pavement Research and Technology [Preprint], 2022. https://doi.org/10.1007/s42947-022-00214-6.

49. i, C. *et al.* Performance assessment and comparison of two piezoelectric energy harvesters developed for Pavement Application: Case Study. Sustainability, 14(2): 863, 2022. https://doi.org/10.3390/su14020863.

50. Pan, Q. *et al.* Field measurement of strain response for typical asphalt pavement. Journal of Central South University, 28(2): 618–632, 2021. https://doi.org/10.1007/s11771-021-4626-9.

51. Liu, P. *et al.* Numerical Study on influence of Piezoelectric Energy Harvester on asphalt pavement structural responses. Journal of Materials in Civil Engineering, 31(3), 2019. https://doi.org/10.1061/(ASCE)MT.1943-5533.0002640.

52. Bezabih, A. & Chandra, S. Comparative study of flexible and rigid pavements for different soil and traffic conditions Journal of the Indian Roads Congress, 3: 153-162, 2009. https://doi.org/10.26682/csjuod.2020.23.2.18.

53. Nega, A. and Nikraz, H. Evaluation of tire-pavement contact stress distribution of pavement response and some effects on the flexible pavements. Airfield and Highway Pavements 2017 [Preprint]. https://doi.org/10.1061/9780784480946.

54. Trnka, L. and Gogola, M. Analysis of the tire contact area pressure on the road. Perner's Contacts, 19(2), 2019. (n/d)

55. Gupta, A. and Kumar, A. Comparative structural analysis of flexible pavements using finite element method. International Journal on Pavement Engineering & Asphalt Technology, 15(1): 11–19, 2014. https://doi.org/10.2478/ijpeat-2013-0005.

56. Roshani, H. *et al.* Theoretical and experimental evaluation of two roadway piezoelectric-based energy harvesting prototypes. Journal of Materials in Civil Engineering, 30(2), 2018. https://doi.org/10.1061/(ASCE)MT.1943-5533.0002112.

57. Yuan, H. *et al.* Design of piezoelectric device compatible with pavement considering traffic: Simulation, laboratory and on-site. Applied Energy, 306: 118153, 2022. https://doi.org/10.1016/j.apenergy.2021.118153.

58. Yang, H. *et al.* Development of Piezoelectric Energy Harvester system through optimizing multiple structural parameters. Sensors, 21(8): 2876, 2021. https://doi.org/10.3390/s21082876.

59. Cao, Y. *et al.* Electric energy output model of a piezoelectric transducer for pavement application under vehicle load excitation. Energy, 211: 118595, 2020. https://doi.org/10.1016/j.energy.2020.118595.

60. Cao, Y., Zhang, F., *et al.* Energy conversion models and characteristics under various inner connections of a novel packaged piezoelectric transducer for pavements. Energy Conversion and Management, 245: 114563, 2021. https://doi.org/10.1016/j.enconman.2021.114563.

61. Lv, J. *et al.* Finite element analysis of piezoelectric stack transducer embedded in asphalt pavement. 2015 Symposium on Piezoelectricity, Acoustic Waves, and Device Applications (SPAWDA) [Preprint]. https://doi.org/10.1109/SPAWDA.2015.7364461.

62. Wang, C. *et al.* Structure simulation optimization and test verification of Piezoelectric Energy Harvester device for road. Sensors and Actuators A: Physical, 315: 112322, 2020. https://doi.org/10.1016/j.sna.2020.112322.

63. Omnexus, (2023) Polyamide (PA) or Nylon: Complete Guide (PA6, PA66, PA11, PA12...), Polyamide/Nylon (PA): Uses & Properties [Updated 2023]. Available at: https://omnexus.specialchem.com/selection-guide/polyamide-pa-nylon?src=prop-cnx (Accessed: 04 August 2023).

64. "Polyamide (Nylon) Plastic", www.makeitfrom.com/material-group/Polyamide-Nylon-Plastic, retrieved 2023-10-02.

65. Smiths, (no date) 'Extruded Nylon Types 66 & 6'.

66. Haoues, S. *et al.* Modeling and optimization in turning of PA66-GF30% and PA66 using multi-criteria decision making (PSI, MABAC and Mairca) methods: A comparative study. The International Journal of Advanced Manufacturing Technology, 124(1), 2022. https://doi.org/10.21203/rs.3.rs-1952494/v1.

67. Sherren, A. *et al.* Experimental and simulation validation of Piezoelectric Road Energy Harvesting. Open Journal of Energy Efficiency, 11(03): 122–141, 2022. https://doi.org/10.4236/ojee.2022.113009.

68. Schlichting, A.D., Fink, E. and Garcia, E. A low-loss hybrid rectification technique for piezoelectric energy harvesting. Smart Materials and Structures, 229: 095028, 2013. https://doi.org/10.1088/0964-1726/22/9/095028.

69. Edla, M. *et al.* An improved self-powered H-bridge circuit for voltage rectification of Piezoelectric Energy Harvesting System. IEEE Journal of the Electron Devices Society, 8: 1050–1062, 2020. https://doi.org/10.1109/jeds.2020.3025554.

70. Edla, M. *et al.* An improved rectifier circuit for piezoelectric energy harvesting from human motion. Applied Sciences, 11(5): 2008, 2021. https://doi.org/10.3390/app11052008.

71. Schlichting, A.D., Fink, E. and Garcia, E. A low-loss hybrid rectification technique for piezoelectric energy harvesting. Smart Materials and Structures, 22(9): 095028, 2013. https://doi.org/10.1088/0964-1726/22/9/095028.

72. Hu, Y., Xue, H. and Hu, H. A piezoelectric power harvester with adjustable frequency through axial preloads. Smart Materials and Structures, 16(5): 1961–1966, 2007. https://doi.org/10.1088/0964-1726/16/5/054.

73. Common substances, materials, foods and Gravels (nd) https://www.aqua-calc.com/page/density-table

74. Yang, H. *et al.* A preliminary study on the highway piezoelectric Power Supply System', International Journal of Pavement Research and Technology, 11(2): 168–175, 2018. https://doi.org/10.1016/j.ijprt.2017.08.006.

75. Guo, L. and Lu, Q. Potentials of piezoelectric and thermoelectric technologies for harvesting energy from pavements. Renewable and Sustainable Energy Reviews, 72: 761–773, 2017. https://doi.org/10.1016/j.rser.2017.01.090.

76. Zhang, W., Ding, G. and Wang, J. Road energy harvesting characteristics of damage-resistant stacked piezoelectric ceramics. Ferroelectrics, 570(1): 37–56, 2021. https://doi.org/10.1080/00150193.2020.1839254.

77. Du, C. *et al.* Finite Element Modeling and performance evaluation of Piezoelectric Energy Harvesters with various piezoelectric unit distributions. Materials, 14(6): 1405, 2021. https://doi.org/10.3390/ma14061405.

78. Du, C. *et al.* Evaluation of the piezoelectric and mechanical behaviors of asphalt pavements embedded with a piezoelectric energy harvester based on multiscale finite element simulations. Construction and Building Materials, 333: 127438, 2022. https://doi.org/10.1016/j.conbuildmat.2022.127438.

79. Yang, H., Wang, L., *et al.* Development in stacked-array-type piezoelectric energy harvester in asphalt pavement. Journal of Materials in Civil Engineering, 29(11), 2017. https://doi.org/10.1061/(ASCE)MT.1943-5533.0002079.

Appendix. Current transducers made in piezoelectric energy harvesters' field for pavements

№	Authors	Piezoelectric material	Transducer protection	Device shape	Bearing plate	Positioning plate	Base plate	Electrodes	Environmental protection	Electrical protection	Additional information
1	58	Stack PZT-5H	NA	Square	PA66-GF 30	Glass fiber	PA66-GF 30	Stainless steel	Silica gel	NA	
2	48	Stack PZT-5H	Protective gaskets	Square	Engineering plastics	Silicon	Engineering plastics	NA	Rubber sponge and glass adhesive	Full-Bridge rectifiers	
3	62	Stack PZT-5	Rubber pad as elastomer material	Square	PP	Fiber	PP	Copper	Silicone rubber film	NA	Fiber has heat insulation properties
4	56	Cylindrical PZT-4	NA	Round	NA	Polystyrene	NA	Copper	NA	NA	
5	19	Stack PZT-5H	Bronze gasket	Square	Aluminum alloy	PA66	PA66	Copper	Silicone rubber film	Full-Bridge rectifiers	
6	76	Stack PZT-554	Fluorine rubber pad	Round	Nylon	Nylon	Nylon	Copper	NA	NA	Nylon for 3D printer was used
7	51	PZT-5H	Stainless steel gasket	Square	PA66-GF 30	PA66-GF 30	PA66-GF 30	NA	Silicone gasket	Rectifiers (not specified)	
8	77 78	Stack PZT-5H	NA	Square	PA66-GF 30	NA	PA66-GF 30	NA	NA	NA	
9	79	Stack PZT-5H	NA	Square	MC Nylon	MC Nylon	MC Nylon	NA	NA	Full-Bridge rectifiers	
10	66	Stack PZT-53HD	NA	Round	Polycarbonate	PLA	Polycarbonate	NA	Neoprene Rubber	NA	1018 AISI low carbon steel base plate
11	59	Cylindrical PZT-5H	Shim	Round	Engineering plastics	Engineering plastics	Engineering plastics	Copper	NA	NA	Full-pressure concept
12	61	Stack PZT-8	NA	Round	Nylon	NA	Nylon	Copper	NA	NA	
13	74	Stack PZT-5H	Stainless steel gasket	Square	PA66-GF 30	PA66-GF 30	PA66-GF 30	Copper	Silicon gasket	Full-Bridge rectifiers	